Geophysical Prospecting

EAGE EUROPEAN ASSOCIATION OF GEOSCIENTISTS & ENGINEERS

Geophysical Prospecting, 2018, **66**, 85–97 doi: 10.1111/1365-2478.12530

Data-driven time–frequency analysis of seismic data using non-stationary Prony method

Guoning Wu[1]*, Sergey Fomel[2] and Yangkang Chen[3]

[1]*College of Science, China University of Petroleum, Beijing 102249, China,* [2]*Bureau of Economic Geology, John A. and Katherine G. Jackson School of Geosciences, The University of Texas at Austin, University Station, Box X, Austin, TX 78731-8924 USA, and* [3]*Oak Ridge National Laboratory, Oak Ridge, TN 37830 USA*

Received October 2016, revision accepted March 2017

ABSTRACT

Empirical mode decomposition aims to decompose the input signal into a small number of components named intrinsic mode functions with slowly varying amplitudes and frequencies. In spite of its simplicity and usefulness, however, empirical mode decomposition lacks solid mathematical foundation. In this paper, we describe a method to extract the intrinsic mode functions of the input signal using non-stationary Prony method. The proposed method captures the philosophy of the empirical mode decomposition but uses a different method to compute the intrinsic mode functions. Having the intrinsic mode functions obtained, we then compute the spectrum of the input signal using Hilbert transform. Synthetic and field data validate that the proposed method can correctly compute the spectrum of the input signal and could be used in seismic data analysis to facilitate interpretation.

Key words: time-frequency analysis, non-stationary Prony method, intrinsic mode function, Hilbert transform.

INTRODUCTION

Time–frequency analysis maps a 1D time signal into 2D time and frequency domains, which can capture the non-stationary character of seismic data. Time–frequency analysis is a fundamental tool for seismic data analysis and geological interpretation (Castagna, Sun and Siegfried 2003; Reine, van der Baan and Clark 2009; Chen *et al.* 2014; Liu, Cao and Chen 2016). Conventional time–frequency methods such as short-time Fourier transform (Cohen 1989), wavelet transform (Mallat 1989), and S-transform (Stockwell, Mansinha and Lowe 1996) are under the control of Heisenberg/Gabor uncertainty principle, which states that we cannot have the energy arbitrarily located in both time and frequency domains (Mallat 2009). Moreover, short-time Fourier transform, wavelet transform, and S-transform are using a windowing process, which often brings smearing and leakage (Tary *et al.* 2014). Therefore, spurious frequencies are often generated, which will "colour" the real time–frequency map and affect the interpretation. In recent years, many new methods have been proposed, such as matching pursuit (Mallat and Zhang 1993), basis pursuit (Chen, Donoho and Saunders 1998), empirical mode decomposition (Huang *et al.* 1998; Chen and Fomel 2015), and the synchrosqueezing wavelet transform (Daubechies, Lu and Wu 2011) and its variants such as the synchrosqueezing short-time Fourier transform (Oberlin, Meignen and Perrier 2014) and the synchrosqueezing S-transform (Huang *et al.* 2015). The matching pursuit and basis pursuit methods represent the energies of the input signal by the energies of atoms found using different methods, which prevents smearing and leakage, creating highly localised time–frequency decompositions. The efficiency of these two methods depends on a predefined dictionary (Tary *et al.* 2014). The empirical mode decomposition method decomposes a signal into symmetric, narrow-band waveforms named intrinsic mode functions to compress artificial spectra caused by sudden changes and, therefore, to improve the time–frequency resolution (Han and van der Baan 2013).

*E-mail: wuguoning@gmail.com

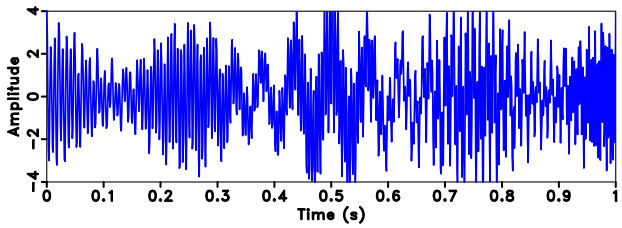

Figure 1 Synthetic signal.

However, the empirical mode decomposition method also suffers from mode mixing and splitting problems. In order to solve the aforementioned problems, alternative methods were developed based on empirical mode decomposition, i.e., ensemble empirical mode decomposition (Wu and Huang 2009) and complete ensemble empirical mode decomposition (Torres *et al.* 2011). However, these two methods, like the empirical mode decomposition method, are still "empirical" because of their sketchy mathematical justifications. The synchrosqueezing wavelet transform (Daubechies *et al.* 2011) and its variants capture the philosophy of empirical mode decomposition, but, use a different method to compute the intrinsic mode functions, providing a rigorous mathematical framework.

Similar to the Fourier transform, the Prony method (Prony 1795) decomposes a signal into a series of damped exponentials or sinusoids in a data-driven manner, which allows for the estimation of frequencies, amplitudes, phases, and damping components of a signal. Fomel (2013) proposed the non-stationary Prony method (NPM) based on regularised non-stationary autoregression. The NPM decomposes a signal into intrinsic mode functions with controlled smoothness of amplitudes and frequencies like the empirical mode decomposition does but uses NPM instead. Unlike the Fourier transform, the coefficients of the extracted intrinsic mode functions for the Prony method do not clearly define the energy distribution for the input signal in the time–frequency domain. Therefore, the NPM used by Fomel does not clearly define a "real" time–frequency map but a "time-component" map. In this paper, we couple the NPM (Fomel 2013) and the Hilbert transform to give a time–frequency decomposition. The proposed method has a rigorous mathematical framework. Furthermore, synthetic and real data tests confirm that the intrinsic mode functions derived by the proposed method

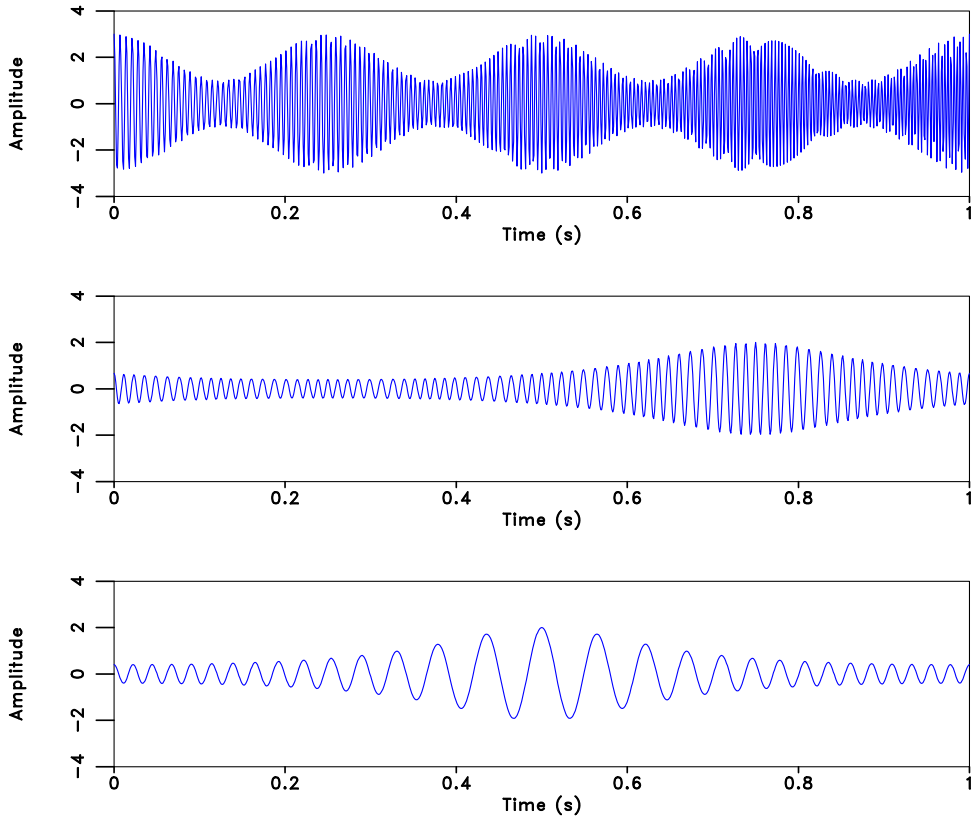

Figure 2 Components of the synthetic signal in Fig. 1.

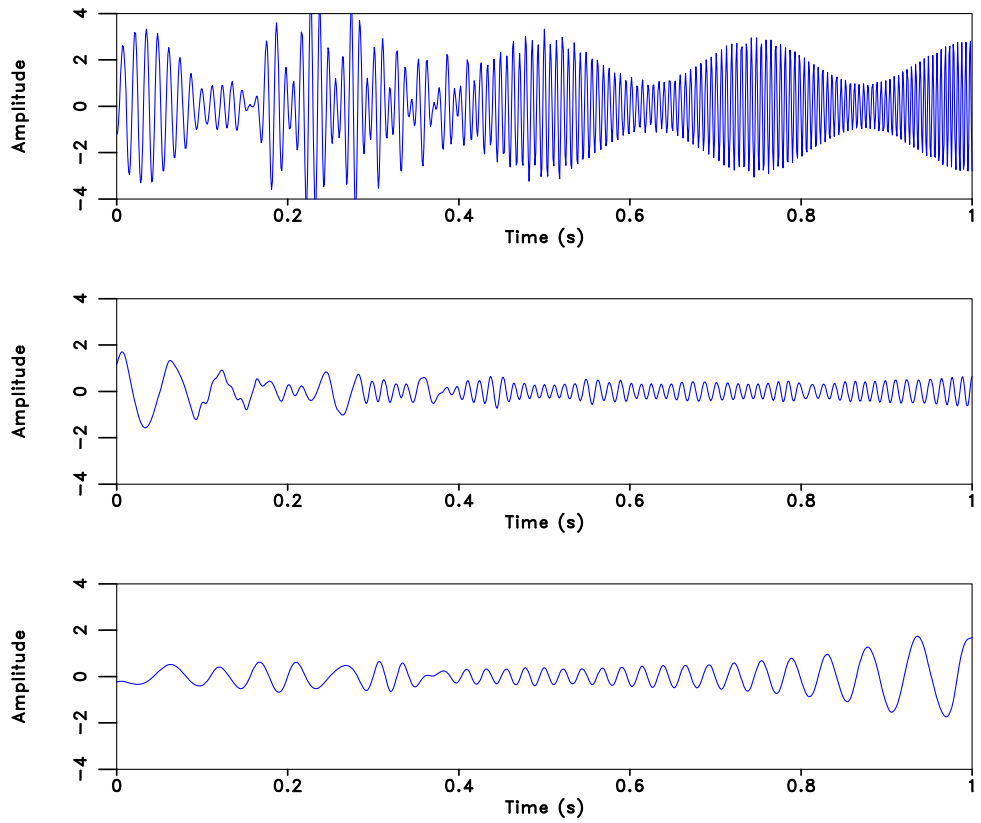

Figure 3 Components of the synthetic signal in Fig. 1 using ensemble empirical mode decomposition.

are smoother with respect to the amplitudes and frequencies than the intrinsic mode functions of ensemble empirical mode decomposition (Wu and Huang 2009). Synthetic and real data tests also confirm that the proposed method has a higher time–frequency resolution than the ensemble empirical mode decomposition method. The proposed method can be used to facilitate seismic interpretation.

THEORY

We give a short description of the theories for the empirical mode decomposition and Prony methods and the non-stationary Prony method (NPM). For details of the NPM and the Prony method, see the Appendix.

Empirical mode decomposition

Empirical mode decomposition is a data-driven method, which is a powerful tool for non-stationary signal analysis (Huang *et al.* 1998). This method decomposes a signal into slowly varying time-dependent amplitude and phase components named intrinsic mode functions. The time–frequency decomposition for the input signal is attributed to the Hilbert transform of the intrinsic mode functions extracted by sifting process (Han and van der Baan 2013). If $s(t)$ is the input signal, empirical mode decomposition can be written as follows:

$$s(t) = \sum_{k=1}^{K} s_k(t) = \sum_{k=1}^{K} A_k(t)\cos(\phi_k(t)), \tag{1}$$

where $A_k(t)$ measures amplitude modulation and $\phi_k(t)$ measures phase oscillation. Each $s_k(t)$ has a narrow-band waveform and an instantaneous frequency that is smooth and positive. The empirical mode decomposition method is powerful, but its mathematical theory is sketchy.

Prony method

Prony method extracts damped complex exponential functions (or sinusoids) from a given signal by solving a set of linear equations (Prony 1795; Lobos, Rezmer and Schegner 2003; Peter and Plonka 2013; Mitrofanov and Priimenko 2015). The Prony method allows for the estimation of frequencies, amplitudes, and phases of a signal (For details, see

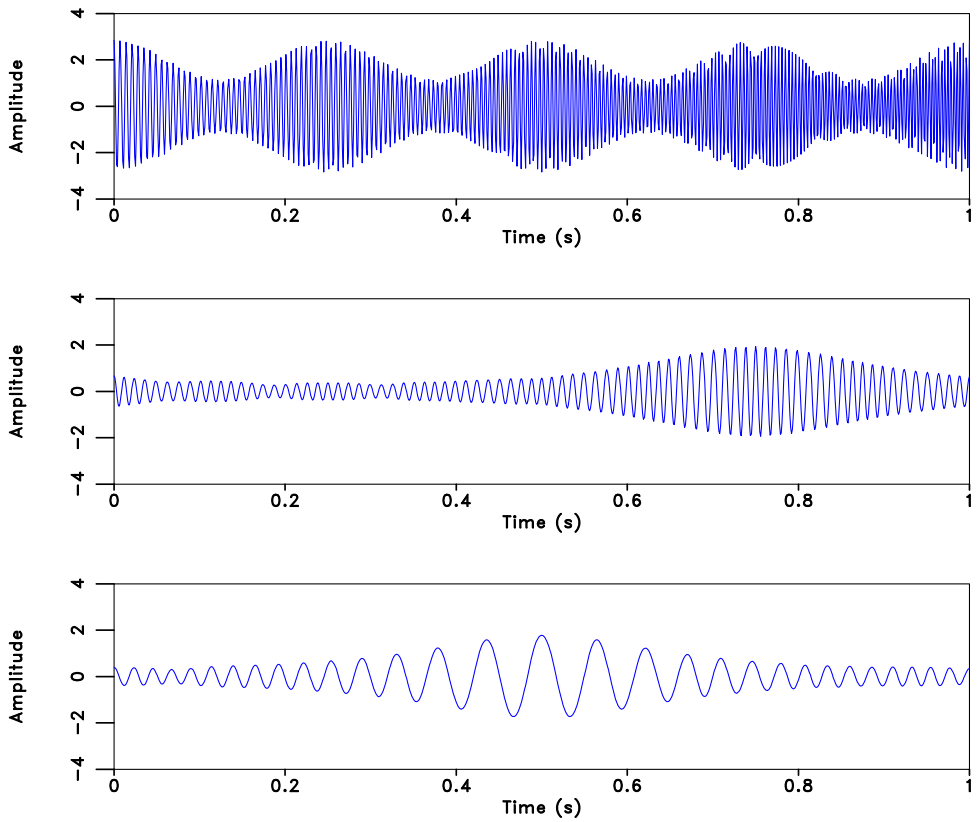

Figure 4 Components of the synthetic signal in Fig. 1 using NPM.

the Appendix.) Assume that we want to solve the following problem:

$$x[n] = \sum_{k=1}^{M} A_k e^{(\alpha_k + j\omega_k)(n-1)\Delta t + j\phi_k}. \tag{2}$$

If we let $h_k = A_k e^{j\phi_k}$, $z_k = e^{(\alpha_k + j\omega_k)\Delta t}$, we derive the concise form

$$x[n] = \sum_{k=1}^{M} h_k z_k^{n-1}. \tag{3}$$

The above M equations can be written in the following matrix form:

$$\begin{bmatrix} z_1^0 & z_2^0 & \cdots & z_M^0 \\ z_1^1 & z_2^1 & \cdots & z_M^1 \\ \vdots & \vdots & & \vdots \\ z_1^{M-1} & z_2^{M-1} & \cdots & z_M^{M-1} \end{bmatrix} \begin{bmatrix} h_1 \\ h_2 \\ \vdots \\ h_M \end{bmatrix} = \begin{bmatrix} x[1] \\ x[2] \\ \vdots \\ x[M] \end{bmatrix}. \tag{4}$$

The above $z_k, k = 1, 2, \cdots, M$ of equation (4) can be computed by solving a polynomial of the form

$$P(z) = \prod_{k=1}^{M} (z - z_k). \tag{5}$$

Equation (5) can also be written in the following form:

$$P(z) = a_0 z^M + a_1 z^{M-1} + \cdots + a_{M-1} z + a_M. \tag{6}$$

The coefficients a_k of the polynomial can be computed by solving the following equation:

$$\sum_{m=0}^{M} a_m x[n-m] = 0. \tag{7}$$

We use the method proposed by Toh and Trefethen (1994) to compute the roots z_k of equation (6). If the roots are solved, h_k can be computed using equation (3). Finally, the components are computed based on the following equation (see the Appendix):

$$c_k[n] = h_k z_k^{n-1} = h_k z_k^{n-1}, k = 1, 2, \cdots, M. \tag{8}$$

Non-stationary Prony method

Equation (7) can be written as follows:

$$\sum_{m=1}^{M} \hat{a}_m x[n-m] = x[n]. \tag{9}$$

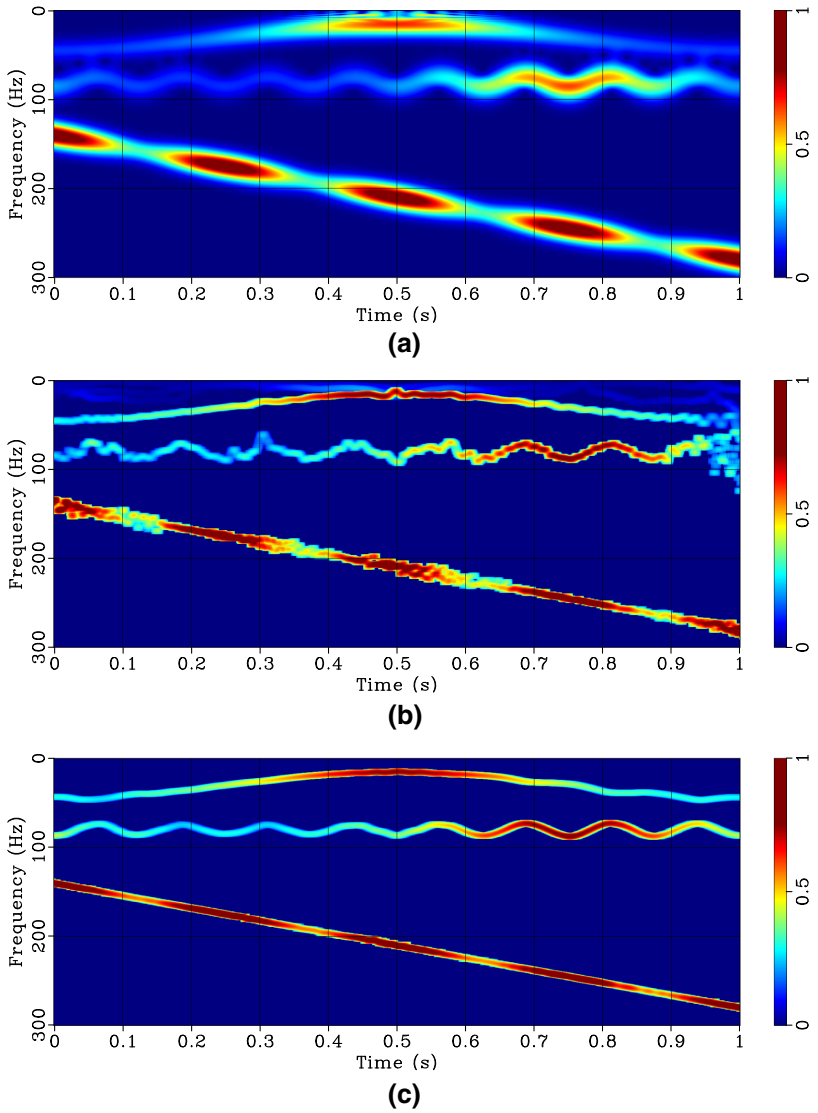

Figure 5 (a) Time–frequency map for the synthetic signal in Fig. 1 using local attribute. (b) Time–frequency map for the synthetic signal in Fig. 1 using ensemble empirical mode decomposition. (c) Time–frequency map for the synthetic signal in Fig. 1 using the proposed method.

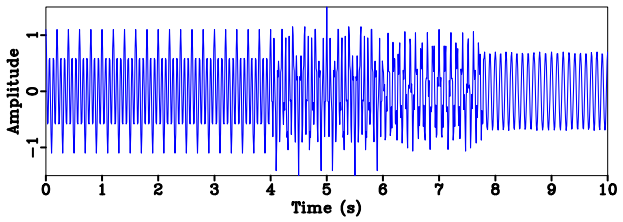

Figure 6 Synthetic signal.

If $\hat{a}_m$ in equation (9) are time dependent, then we have

$$\sum_{m=1}^{M} \hat{a}_m[n]x[n-m] \approx x[n], \tag{10}$$

which is an underdetermined linear system. There are many methods for solving underdetermined linear systems, such as Tikhonov method (Tikhonov 1963). In this paper, we apply shaping regularization (Fomel 2007, 2009) to regularise the underdetermined linear system and obtain (see the Appendix):

$$\hat{\mathbf{a}} = \mathbf{F}^{-1}\boldsymbol{\eta}, \tag{11}$$

where $\hat{\mathbf{a}}$ is a vector composed of $\hat{a}_m[n]$, and the elements of vector $\boldsymbol{\eta}$ are $\eta_i[n] = \mathbf{S}[x_i^*[n]x[n]]$, where $x_i[n] = x[n-i]$, $x_i^*[n]$ stands for the complex conjugate of $x_i[n]$ and $\mathbf{S}$ is the shaping operator. The elements of matrix $\mathbf{F}$ are as follows:

$$F_{ij}[n] = \sigma^2\delta_{ij} + \mathbf{S}\left[x_i^*[n]x_j[n] - \sigma^2\delta_{ij}\right], \tag{12}$$

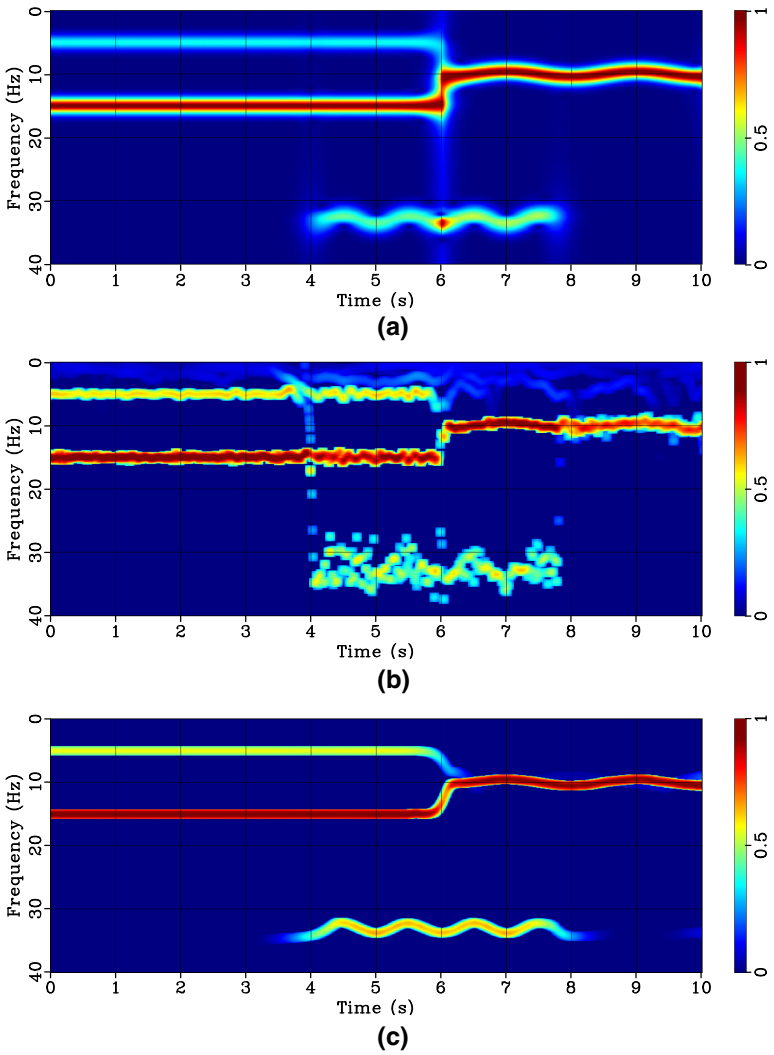

Figure 7 (a) Time–frequency map for the synthetic signal in Fig. 6 using local attribute. (b) Time–frequency map for the synthetic signal in Fig. 6 using ensemble empirical mode decomposition. (c) Time–frequency map for the synthetic signal in Fig. 6 using the proposed method.

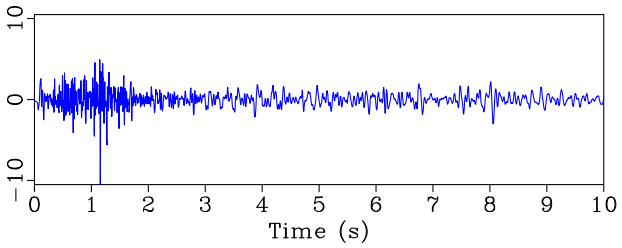

Figure 8 Seismic trace from marine survey.

where σ is the regularization parameter. Solving equation (11), we obtain the coefficients' vector $\hat{a}_m[n]$ and form a polynomial as follows:

$$P(z) = z^M + \hat{a}_1[n]z^{M-1} + \cdots + \hat{a}_M[n]. \tag{13}$$

For the root computation $\hat{z}_m[n], m = 1, 2, \ldots, M$ of the above polynomial, we use the method proposed by Toh and Trefethen (1994). The instantaneous frequency of each different component is derived from the following equation:

$$f_m[n] = \Re\left[\arg\left(\frac{\hat{z}_m[n]}{2\pi\,\Delta t}\right)\right]. \tag{14}$$

From the instantaneous frequency, we compute the local phase according to the following equation:

$$\Phi_m[n] = 2\pi \sum_{k=0}^{n} f_m[k]\Delta t. \tag{15}$$

Solve the following equation using a regularised non-stationary regression method (Fomel 2013):

$$x[n] = \sum_{m=1}^{M} \hat{A}_m[n]\mathrm{e}^{i\Phi_m[n]} = \sum_{m=1}^{M} c_m[n]. \tag{16}$$

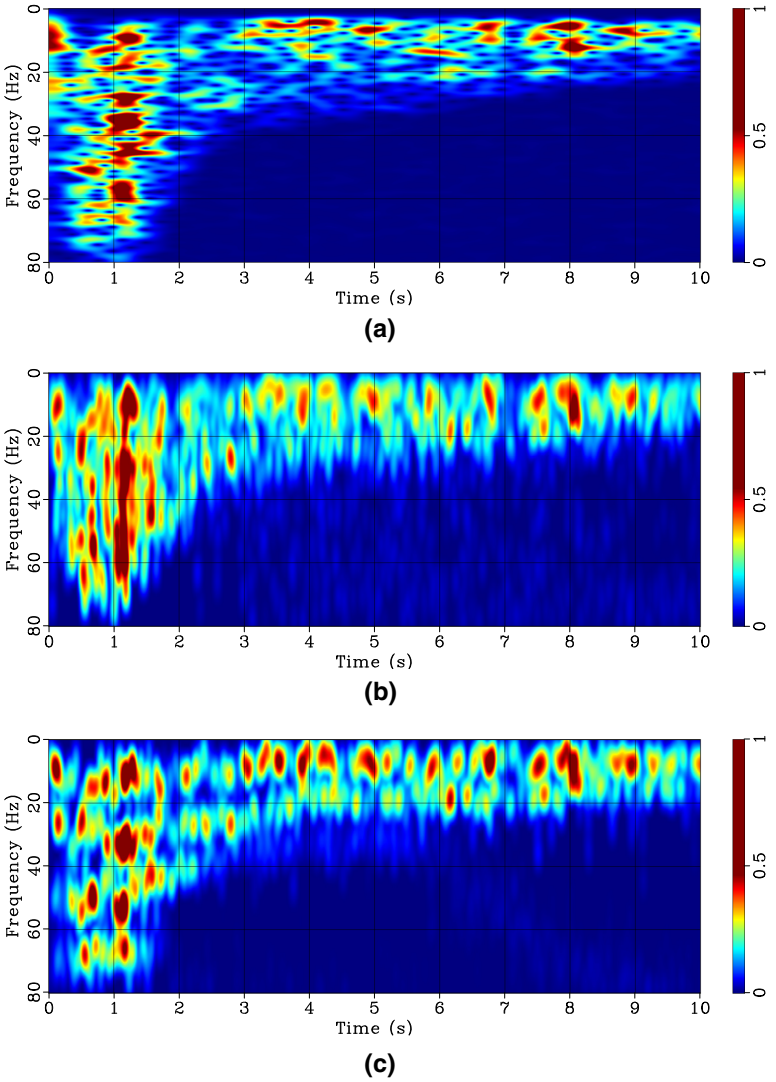

Figure 9 (a) Time–frequency map for the synthetic signal in Fig. 8 using local attribute. (b) Time–frequency map for the synthetic signal in Fig. 8 using ensemble empirical mode decomposition. (c) Time–frequency map for the synthetic signal in Fig. 8 using the proposed method.

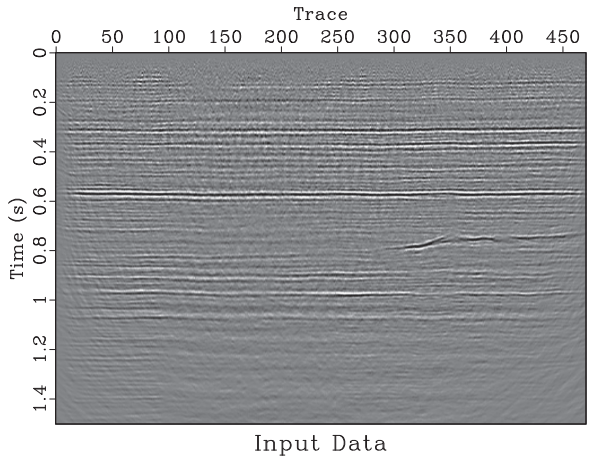

Figure 10 Two-dimensional seismic data section.

Finally, the narrow-band intrinsic mode functions $c_m[n]$ are computed based on equation (16)

EXAMPLES

We use synthetic signals and real field data to test the proposed method.

Benchmark examples

We use a simple synthetic signal to test the proposed method. Figure 1 is a synthetic signal from Hou and Shi (2013). The three components of the signal are shown in Fig. 2. Figures 3 and 4 show the intrinsic mode functions extracted by the ensemble empirical mode decomposition method and the

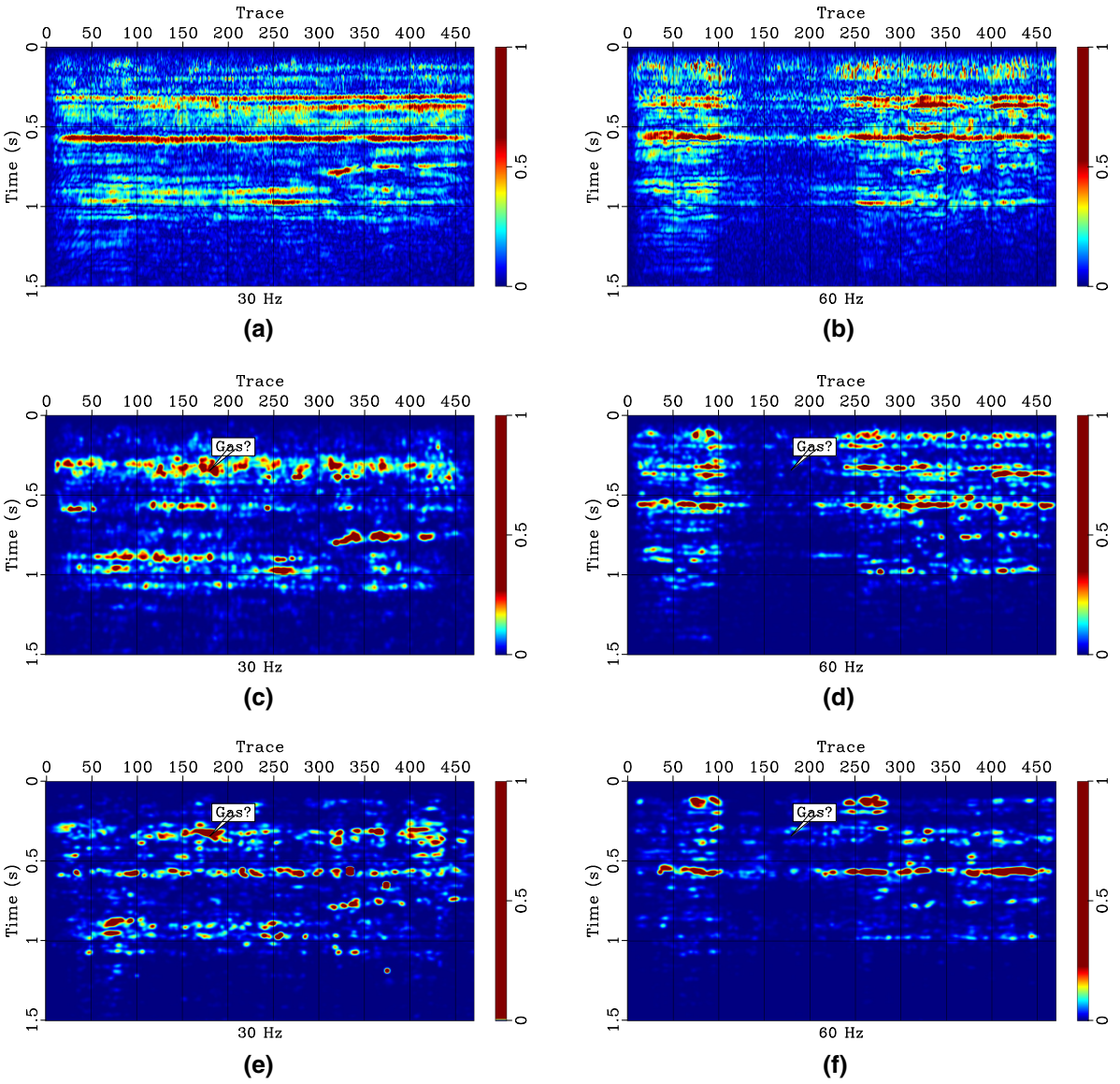

Figure 11 (a) 30-Hz slice time–frequency map using the local attribute method. (b) 60-Hz slice time–frequency map using the local attribute method. (c) 30-Hz slice time–frequency map using the ensemble empirical mode decomposition method. (d) 60-Hz slice time–frequency map using the ensemble empirical mode decomposition method. (e) 30-Hz slice time–frequency map of the proposed method. (f) 60-Hz slice time–frequency map of the proposed method.

non-stationary Prony method (NPM). From the figures, we see that the NPM accurately identifies the three components that the signal has. The intrinsic mode functions derived by the NPM are smoother with respect to amplitudes and frequencies compared with the intrinsic mode functions obtained by ensemble empirical mode decomposition. For ensemble empirical mode decomposition, we repeat the empirical mode decomposition 25 times with different levels of noise to generate the ensemble empirical mode decomposition results. The time–frequency distributions of the input signal are the Hilbert transform of the intrinsic mode functions. Figure 5 a–c shows the time–frequency distributions using local attribute (Liu, Fomel and Chen 2011), ensemble empirical mode decomposition (Wu and Huang 2009), and the proposed method for the synthetic signal in Fig. 1, respectively. Figure 6 shows another synthetic signal. Figure 7 a–c shows the time–frequency maps using local attribute (Liu *et al.* 2011), ensemble empirical mode decomposition (Wu and Huang 2009), and the

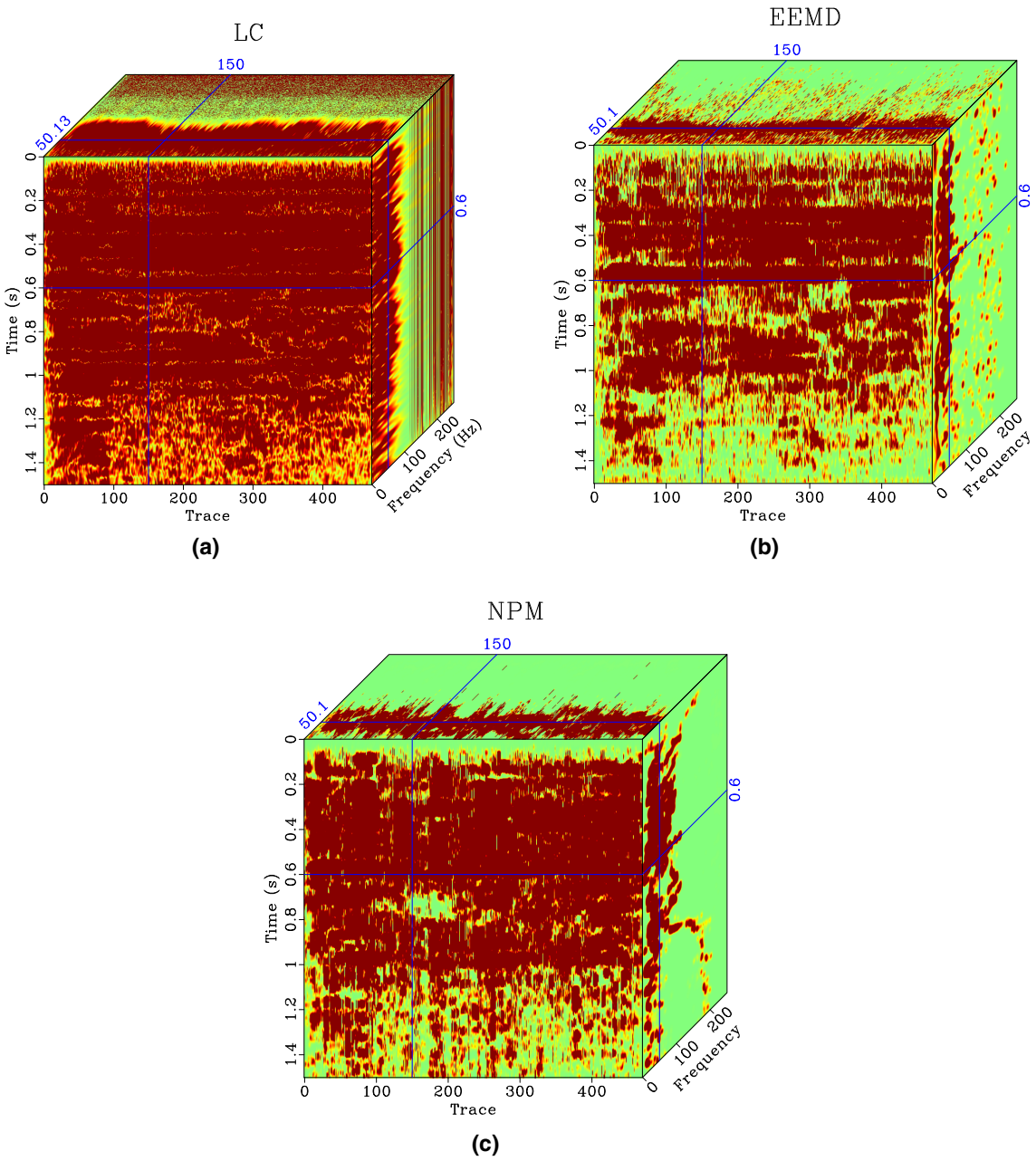

Figure 12 (a) Time–frequency cube using the local attribute method. (b) Time–frequency cube using the ensemble empirical mode decomposition method. (c) Time–frequency cube using the NPM.

proposed method. From the figures, we see that the energy is compactly spread over the instantaneous frequencies for the ensemble empirical mode decomposition method. However, the energy is not steadily distributed for the ensemble empirical mode decomposition method. The proposed method provides a steady and compact energy distribution, which sharpens the time–frequency distribution.

Field examples

Figure 8 is a seismic trace from marine survey. Figure 9 a–c shows the time–frequency distributions of the trace using local attribute (Liu *et al.* 2011), ensemble empirical mode decomposition, and the proposed method. We can see that the energy distributions for ensemble empirical mode decomposition and the proposed method are much like each other. Both the

ensemble empirical mode decomposition and proposed methods use the Hilbert transform of the intrinsic mode functions to represent the time–frequency distributions for the input signal. The results confirm that they both reveal the time–frequency character of the input signal.

Low-frequency anomalies are often attributed to abnormally high attenuation in gas-filled reservoirs and can be used as a hydrocarbon indicator (Castagna *et al.* 2003). The mechanisms of low-frequency anomalies associated with hydrocarbon reservoirs are not clearly understood (Ebrom 2004; Kazemeini *et al.* 2009). Figure 10 shows 2D field seismic data. Figure 11a and b, 11c and d, and 11e and f shows the 30- and 60-Hz constant frequency slices using local attribute, ensemble empirical mode decomposition, and the proposed method, respectively. From the these figures, we see that there is a low-frequency anomaly in the upper left part of the data section indicated by the text boxes "Gas?" for the ensemble empirical mode decomposition and the proposed methods, which may correspond to gas presentation.

Figure 12a–c shows the full time–frequency cubes computed using local attribute, ensemble empirical mode decomposition, and the proposed methods, respectively. The main panels show constant frequency slices. The right-hand-side panels show the time–frequency maps of the 150th trace. The top panels show the time–frequency maps of 0.6-second time–depth signal. From the right and top side panels, we see that there is a lot of noise in the high-frequency domain for the ensemble empirical mode decomposition and local attribute methods compared with the proposed method.

CONCLUSION

We have to compute the time–frequency map of an input signal based on the non-stationary Prony method (NPM) coupled with Hilbert spectral analysis. The proposed method is an empirical mode decomposition-like method but uses NPM to compute its intrinsic mode functions. Compared with the Fourier transform, the proposed method is data driven and needs much less base functions to approximate the original signal. Since the NPM results in an underdetermined linear system, we use shaping regularization to regularise it. Regularization makes the intrinsic mode functions smoother with respect to the amplitudes and frequencies compared with the intrinsic mode functions of the empirical mode decomposition. There are many time–frequency methods, but which one is the best? This is a difficult question to answer. Methods are good for some type of signals but maybe not good for other type of signals.

Wang *et al.* (2014) pointed out that the complexity of empirical mode decomposition/ensemble empirical mode decomposition is $41N_E N_S n(\log_2 n) = O(n \log n)$, where n is the data length and parameters N_E and N_S are the ensemble and sifting numbers, respectively. For the NPM, the computation complexity is mainly attributed to the polynomial zero finding. We used the pseudo-zeros method to compute the pseudo-spectra of the associated balanced companion matrix (Toh and Trefethen 1994), which requires approximate N^3 works, where N is the polynomial degree number. Therefore, the total computation complexity is $N^3 \frac{n}{N} = nN^2$, where n is the data length. In this paper, we choose $N = 5$, and therefore, the total computation complexity is approximately $5n^2 = O(n)$.

ACKNOWLEDGEMENTS

The authors would like to thank Zhiguang Xue and Junzhe Sun for their constructive suggestions. The first author would like to thank China University of Petroleum-Beijing for supporting his visit to the Bureau of Economic Geology at The University of Texas at Austin. The work is partially supported by the Youth Science Foundation of China University of Petroleum at Beijing (Grant 01jb0508) and the Science Foundation of China University of Petroleum-Beijing (Grant 2462015YQ0604).

REFERENCES

Castagna J., Sun S. and Siegfried R.W. 2003. Instantaneous spectral analysis: detection of low-frequency shadows associated with hydrocarbons. *The Leading Edge* **22**, 120–127.

Chen S.S., Donoho D.L. and Saunders M.A. 1998. Atomic decomposition by basis pursuit. *SIAM Review* **20**(1), 33–61.

Chen Y. and Fomel S. 2015. EMD-seislet transform. 85th SEG annual international meeting, Expanded Abstracts, 4775–4778.

Chen Y., Liu T., Chen X., Li J. and Wang E. 2014. Time-frequency analysis of seismic data using synchrosqueezing wavelet transform. *Journal of Seismic Exploration* **23**(4), 303–312.

Cohen L. 1989. Time-frequency distributions—A review. *Proceedings of the IEEE* **77**(7), 941–981.

Daubechies I., Lu J. and Wu H.T. 2011. Synchrosqueezed wavelet transforms: an empirical mode decomposition-like tool. *Applied and Computational Harmonic Analysis* **30**(2), 243–261.

Ebrom D. 2004. The low frequency gas shadows in seismic sections. *The Leading Edge* **23**, 772.

Fomel S. 2007. Shaping regularization in geophysical estimation problems. *Geophysics* **72**(2), R29–R36.

Fomel S. 2009. Adaptive multiple subtraction using regularized nonstationary regression. *Geophysics* **74**(1), V25–V33.

Fomel S. 2013. Seismic data decomposition into spectral components using regularized nonstationary autoregression. *Geophysics* **78**(6), O69–O76.

Han J. and van der Baan M. 2013. Empirical mode decomposition for seismic time-frequency analysis. *Geophysics* **78**(2), O9–O19.

Hou T.Y. and Shi Z. 2013. Data-driven time-frequency analysis. *Applied and Computational Harmonic Analysis* **35**(2), 284–308.

Huang N.E., Shen Z., Long S.R., Wu M.C., Shih H.H., Zheng Q. *et al.* 1998. The empirical mode decomposition and the Hilbert spectrum for nonlinear and non-stationary time series analysis. *Proceedings of the Royal Society of London Series A* **454**, 903–995.

Huang Z., Zhang J., Zhao T. and Sun Y. 2015. Synchrosqueezing S-transform and its application in seismic spectral decomposition. *IEEE Transactions on Geoscience and Remote Sensing* **54**(2), 817–825.

Kazemeini S.H., Juhlin C., Jorgensen K.Z. and Norden B. 2009. Application of the continuous wavelet transform on seismic data for mapping of channel deposits and gas detection at the CO2SINK site, Ketzin, Germany. *Geophysical Prospecting* **57**(1), 111–123

Liu G., Fomel S. and Chen X. 2011. Time-frequency analysis of seismic data using local attributes. *Geophysics* **76**(1), P23–P34.

Liu W., Cao S. and Chen Y. 2016. Seismic time-frequency analysis via empirical wavelet transform. *IEEE Geoscience and Remote Sensing Letters* **13**(1), 28–32.

Lobos T., Rezmer J. and Schegner J. 2003. Parameter estimation of distorted signals using Prony method. *Power Tech Conference Proceedings*, 41–44.

Mallat S. 2009. *A Wavelet Tour of Signal Processing: The Sparse Way*. Academic Press.

Mallat S. and Zhang Z. 1993. Matching pursuit with time-frequency dictionaries. *IEEE Transactions on Signal Processing* **41**(12), 3397–3415.

Mallat S.G. 1989. A theory for multiresolution signal decomposition: the wavelet representation. *IEEE Transactions on Pattern Analysis and Machine Intelligence* **11**(7), 674–693.

Mitrofanov G. and Priimenko V. 2015. Prony filtering of seismic data. *Acta Geophysica* **63**(3), 652–678.

Oberlin T., Meignen S. and Perrier V. 2014. The Fourier-based synchrosqueezing transform. *Proceedings of the IEEE International Conference on Acoustics, Speech and Signal Processing*, 315–319.

Peter T. and Plonka G. 2013. A generalized Prony method for reconstruction of sparse sums of eigenfunctions of linear operators. *Inverse Problems* **29**(2), 025001.

Prony R. 1795. Essai expérimental et analytique. *Annuaire de l'École Polytechnique* **1**(2), 24.

Reine C., van der Baan M. and Clark R. 2009. The robustness of seismic attenuation measurements using fixed- and variable-window time-frequency transforms. *Geophysics* **74**(2), 123–135.

Stockwell R.G., Mansinha L. and Lowe R.P. 1996. Localization of the complex spectrum. *IEEE Transactions on Signal Processing* **44**(4), 998–1001.

Tary J.B., Herrera R.H., Han J. and van der Baan M. 2014. Spectral estimation—What is new? What is next? *Reviews of Geophysics* **52**(4), 723–749.

Tikhonov A.N. 1963. Solution of incorrectly formulated problems and the regularization method. *Soviet Mathematics - Doklady* **4**, 1035–1038.

Toh K. and Trefethen L. 1994. Pseudozeros of polynomials and pseudospectra of companion matrices. *Numerische Mathematik* **68**(3), 403–425.

Torres M.E., Colominas M.A., Schlotthauer G. and Flandrin P. 2011. A complete ensemble empirical mode decomposition with adaptive noise. *Proceedings of the IEEE International Conference on Acoustics, Speech and Signal Processing*, 4144–4147. IEEE.

Wang Y.H., Yeh C.H., Young H.W.V., Hu K. and Lo M.T. 2014. On the computational complexity of the empirical mode decomposition algorithm. *Physica A: Statistical Mechanics and its Applications* **400**(C), 159–167.

Wu Z. and Huang N.E. 2009. Ensemble empirical mode decomposition: a noise-assisted data analysis method. *Advances in Adaptive Data Analysis* **1**(1), 1–41.

APPENDIX

Prony method

Prony method can extract damped complex exponential signals from given data by solving a set of linear equations (Prony 1795; Lobos *et al.* 2003; Peter and Plonka 2013; Mitrofanov and Priimenko 2015). Assume the N complex data samples $x[1], x[2], \cdots x[N]$, we approximate the data by M exponential functions

$$x[n] \approx \sum_{k=1}^{M} A_k \mathrm{e}^{(\alpha_k + \mathrm{j}\omega_k)(n-1)\Delta t + \mathrm{j}\phi_k}, \tag{A-1}$$

where A_k is the amplitude, Δt is the sampling period, α_k is the damping factor, ω_k is the angular frequency, and ϕ_k is the initial phase. If we let $h_k = A_k \mathrm{e}^{\mathrm{j}\phi_k}$, $\mathrm{z_k} = \mathrm{e}^{(\alpha_k + \mathrm{j}\omega_k)\Delta t}$, we then derive the concise form as follows:

$$x[n] \approx \sum_{k=1}^{M} h_k z_k^{n-1}. \tag{A-2}$$

The approximation problem above can be solved based on the error minimisation

$$\min \sum_{n=1}^{N} |\epsilon[n]|^2 = \min \sum_{n=1}^{N} \left| x[n] - \sum_{k=1}^{M} h_k z_k^{n-1} \right|^2. \tag{A-3}$$

This turns out to be a non-linear problem. It can be solved using Prony method that utilises linear equation solutions. If there are as many data samples as parameters of the approximation problem, the above M equation (A-2) can be expressed as follows:

$$x[n] = \sum_{k=1}^{M} h_k z_k^{n-1}. \tag{A-4}$$

Equation (A-4) can be written in a matrix form as as follows:

$$\begin{bmatrix} z_1^0 & z_2^0 & \cdots & z_M^0 \\ z_1^1 & z_2^1 & \cdots & z_M^1 \\ \vdots & \vdots & & \vdots \\ z_1^{M-1} & z_2^{M-1} & \cdots & z_M^{M-1} \end{bmatrix} \begin{bmatrix} h_1 \\ h_2 \\ \vdots \\ h_M \end{bmatrix} = \begin{bmatrix} x[1] \\ x[2] \\ \vdots \\ x[M] \end{bmatrix}. \tag{A-5}$$

Prony proposed to define the polynomial that has the above $z_k, k = 1, 2, \cdots, M$ as its roots (Prony 1795)

$$P(z) = \prod_{k=1}^{M}(z - z_k). \tag{A-6}$$

Equation (A-6) can be rewritten in the following form:

$$P(z) = a_0 z^M + a_1 z^{M-1} + \cdots + a_{M-1} z + a_M. \tag{A-7}$$

Shifting the index on equation (A-4) from n to $n - m$, and multiplying by parameter $a[m]$, we derive

$$\sum_{m=0}^{M} a_m x[n-m] = \sum_{k=1}^{M} h_k z_k^{n-M-1} \sum_{m=0}^{M} a[m] z_k^{M-m}. \tag{A-8}$$

Noticing that $z_k, k = 1, 2, \cdots, M$ are roots of equation (A-7) then equation (A-8) an be written as

$$\sum_{m=0}^{M} a_m x[n-m] = 0. \tag{A-9}$$

Solve equation (A-9) for the polynomial coefficients. In subsequent steps, we compute the frequencies, damping factors, and the phases according to Algorithm 1. After all the parameters are computed, we then compute the components of the input signal. For details, see Algorithm 1 as follows.

Algorithm 1: Prony method

1: *Find coefficients:* $a_k, k = 1, 2, \cdots, M \leftarrow \sum_{m=0}^{M} a_m x[n-m] = 0.$
2: *Find roots:* $z_k, k = 1, 2, \cdots, M \leftarrow \sum_{m=0}^{M} a_m z^{M-m} = 0.$
3: *Compute frequencies:* $\omega_k, k = 1, 2, \cdots, M \leftarrow \Re\{\arg(\frac{z_k}{(k-1)\Delta t})\}, k = 1, 2, \cdots, M.$
4: *Compute:* $A_k e^{\alpha_k (n-1)\Delta t + j\phi_k}, k = 1, 2, \cdots, M \leftarrow x[n] = \sum_{k=1}^{M} A_k e^{(\alpha_k + j\omega_k)(n-1)\Delta t + j\phi_k}.$
5: *Compute components:* $A_k e^{(\alpha_k + j\omega_k)(n-1)\Delta t + j\phi_k}.$

Non-stationary Prony method and shaping regularization

Equation (A-9) can be rewritten as

$$\sum_{m=1}^{M} \hat{a}_m x[n-m] = x[n]. \tag{A-10}$$

If $\hat{a}_m, m = 1, 2, \cdots, M$ in equation (A-10) are time dependent, then we have

$$\sum_{m=1}^{M} \hat{a}_m[n] x[n-m] \approx x[n], \tag{A-11}$$

which is underdetermined. There many methods for solving the underdetermined linear system. For example, Tikhonov (1963) used the regularization method for making the underdetermined problem well-posed by adding constraints on the estimated model.

Shaping regularization

Fomel (2007, 2009) introduces shaping regularization in inversion problem, which regularises the underdetermined linear system by mapping the model to the space of acceptable models. Consider a linear system given as $\mathbf{Fx} = \mathbf{b}$, where $\mathbf{F}$ is the forward modelling map, $\mathbf{x}$ is the model vector, and $\mathbf{b}$ is the data vector. Tikhonov regularization method amounts to minimise the least square problem as follows: (Tikhonov 1963):

$$\min \|\mathbf{Fx} - \mathbf{b}\|^2 + \epsilon^2 \|\mathbf{Dx}\|^2, \tag{A-12}$$

where $\mathbf{D}$ is the regularization operator and ϵ is a scalar parameter. The solution for equation (A-12) is

$$\hat{\mathbf{x}} = (\mathbf{F}^T\mathbf{F} + \epsilon^2 \mathbf{D}^T\mathbf{D})^{-1}\mathbf{F}^T\mathbf{b}, \tag{A-13}$$

where $\hat{\mathbf{x}}$ is the least square approximated of $\mathbf{x}$ and $\mathbf{F}^T$ is the adjoint operator. If the forward operator $\mathbf{F}$ is simply the identity operator, the solution of equation (A-13) is as follows:

$$\hat{\mathbf{x}} = (\mathbf{I} + \epsilon^2 \mathbf{D}^T\mathbf{D})^{-1}\mathbf{b}, \tag{A-14}$$

which can be viewed as a smoothing process. If we let

$$\mathbf{S} = (\mathbf{I} + \epsilon^2 \mathbf{D}^T\mathbf{D})^{-1} \tag{A-15}$$

or

$$\epsilon^2 \mathbf{D}^T\mathbf{D} = \mathbf{S}^{-1} - \mathbf{I}, \tag{A-16}$$

substituting equation (A-16) into equation (A-13) yields a solution by shaping regularization:

$$\hat{\mathbf{x}} = (\mathbf{F}^T\mathbf{F} + \mathbf{S}^{-1} - \mathbf{I})^{-1}\mathbf{F}^T\mathbf{b} = [\mathbf{I} + \mathbf{S}(\mathbf{F}^T\mathbf{F} - \mathbf{I})]^{-1}\mathbf{S}\mathbf{F}^T\mathbf{b}. \tag{A-17}$$

The forward operator **F** may have physical units that require scaling. Introducing scaling λ into **F**, equation (A-17) be written as

$$\hat{\mathbf{x}} = [\lambda^2\mathbf{I} + \mathbf{S}(\mathbf{F}^T\mathbf{F} - \lambda^2\mathbf{I})]^{-1}\mathbf{S}\mathbf{F}^T\mathbf{b}. \tag{A-18}$$

If $\mathbf{S} = \mathbf{H}\mathbf{H}^T$ with square and invertible **H**, equation (A-18) can be written as

$$\hat{\mathbf{x}} = \mathbf{H}[\lambda^2\mathbf{I} + \mathbf{H}^T(\mathbf{F}^T\mathbf{F} - \lambda^2\mathbf{I})\mathbf{H}]^{-1}\mathbf{H}^T\mathbf{F}^T\mathbf{b}. \tag{A-19}$$

The conjugate gradient algorithm can be used for the solution of equation (A-19).

Non-stationary Prony method

Equation (A-11) can be written as a matrix form

$$\sum_{m=1}^{M} \hat{\mathbf{a}}_m(t)\mathbf{x}_m(t) \approx \mathbf{d}(t), \tag{A-20}$$

where $\mathbf{d}(t) = \mathbf{x}(t)$, $\mathbf{x}_m(t) = \mathbf{x}(t - m\Delta t)$ is the time shift of the input signal $\mathbf{x}(t)$ and $\hat{\mathbf{a}}_m(t)$ is the time-dependent coefficient. We solve the underdetermined linear system by using the shaping regularization method. The solution is the following form:

$$\mathbf{a} = \mathbf{F}^{-1}\boldsymbol{\eta}, \tag{A-21}$$

where **a** is a vector of $\hat{a}(t)$, the elements of vector $\boldsymbol{\eta}$ are

$$\boldsymbol{\eta}_i(t) = \mathbf{S}\left[\mathbf{x}_i^*(t)\mathbf{d}(t)\right], \tag{A-22}$$

and the elements of matrix **F** are

$$\mathbf{F}_{ij} = \sigma^2\delta_{ij} + S\left[\mathbf{x}_i^*(t)\mathbf{x}_j(t) - \sigma^2\delta_{ij}\right], \tag{A-23}$$

where σ is the regularization parameter, **S** is a shaping operator, and $\mathbf{x}_i^*(t)$ stands for the complex conjugate of $\mathbf{x}_i(t)$. We can use the conjugate gradient method to find the solution of the linear system. The NPM (Fomel 2013) can be summarised as follows:

Algorithm 2: Non-stationary Prony method

1: *Find time-dependent coefficients using autoregression method:* $\hat{a}_k[n], k = 1, \cdots, M \leftarrow \sum_{m=0}^{M} \hat{a}_m[n]x[n-m] = 0.$
2: *Find time-dependent roots:* $\hat{z}_k[n], k = 1, 2, \cdots, M \leftarrow \sum_{m=0}^{M} \hat{a}_m[n]z^{M-m} = 0.$
3: *Compute time-dependent frequencies:* $\hat{\omega}_k[n], k = 1, \cdots, M \leftarrow \Re\{\arg(\frac{\hat{z}_k[n]}{\Delta t})\}, k = 1, \cdots, M.$
4: *Compute the time-dependent phase:* $\hat{\phi}_k[n] = \sum_{k=0}^{n} \hat{\omega}_k[n]\Delta t.$
5: *Compute components using autoregression method:* $\hat{c}_m[n], m = 1, \cdots M \leftarrow \mathbf{x}[n] \approx \sum_{m=1}^{M} \hat{A}_m[n]e^{i\hat{\phi}_m[n]} = \sum_{m=1}^{M} \hat{c}_m[n]$

After we decompose the input signal into narrow-band components, we compute the time–frequency distribution of the input signal using the Hilbert transform of the intrinsic mode functions.